

Analysis of Oil Behavior inside Rotary Compressor Using Developed Visualization Technique

Pil-Jae Cho, Seung-Kap Lee*, Young Youn*, Han Seo Ko**

Graduate School, Department of Mechanical Engineering, Sungkyunkwan University, Kyunggi-Do 440-746, Korea

*Department of R&D of Rotary Compressor, Samsung Electronics Co., Kyunggi-Do 442-742, Korea

**School of Mechanical Engineering, Sungkyunkwan University, Kyunggi-Do 440-746, Korea

Key words: Rotary compressor, Oil behavior, Quantification, Flow visualization technique, Average intensity

ABSTRACT: An efficiency of a refrigeration cycle and a reliability of a compressor can be reduced if a refrigerant including excessive lubricating oil is exhausted from the compressor. Thus, the analysis of the oil behavior inside the compressor is required to prevent the problem. A tested rotary compressor with visualization windows has been manufactured in this study to investigate the oil behavior using developed visualization techniques. The oil behaviors at various operating conditions have been quantified to obtain the relationship with the outlet pressure inside the compressor. Also, the effect of the operating conditions on the quantity of the exhausted oil from the rotary compressor has been investigated using a manufactured test model.

Nomenclature

I : intensity [%]
 M : number of pixels in horizontal direction of captured image
 N : number of pixels in vertical direction of captured image
 P : pressure
 Q_E : exhausted oil amount [ml]
 Q_I : inserted oil amount [ml]
 Q_R : remained oil amount [ml]
 T_s : inlet temperature of compressor

Subscripts

avg : average
 c : condensation

e : evaporation

1. Introduction

The rotary compressor is widely used for refrigeration systems. However, techniques of reducing exhausted oil have not been studied intensively so far although various researches⁽¹⁾ have been performed for improvement of reliability in a household room air conditioner.

Heat transfer characteristics inside a condenser are influenced by oil which exists in the refrigerant vapor compressed by a compressor. Also, an expansion valve can be frozen if oil is exhausted too much from the compressor. This phenomenon results in reduced efficiency of the expansion valve and an evaporator because an evaporation temperature increases by oil membrane on a heat transfer surface. A total efficiency of the refrigeration cycle also decreases if the oil is discharged too

† Corresponding author

Tel.: +82-31-290-7453; fax: +82-31-290-5889

E-mail address: hanseoko@yurim.skku.ac.kr

much from the compressor because of reduced heat transfer characteristics, pressure drops, and oil deficiency in the compressor. Therefore, the oil behavior should be controlled inside the compressor to improve the reliability of the compressor and the efficiency of the refrigeration cycle.

Techniques of reducing exhausted oil^(2,3) have been developed to date using the oil separation method by reducing the velocity of the refrigerant, improvement of the operating condition, and insertion of a device for oil suppression inside the compressor.⁽⁴⁾ Most researches have studied each lubricating part such as the axis inlet, the journal bearings, and the rotating end of the compression chamber and the suction part.⁽⁵⁻⁷⁾ However, those studies have checked oil flow by the naked eye using the installed visualization window without accurate data of oil behaviors inside the compressor because of the opaque material. Thus, the oil behavior inside the compressor should be analyzed by the quantification of the oil amount to reduce the exhausted oil and design the oil separation system.

In this study, the visualization windows have been installed around the upper part of the rotary compressor to analyze the oil distribution during the operation by the developed visualization and quantification techniques.⁽⁸⁾ Also, a test model has been manufactured to capture the projection of the oil movements by controlling the amount of oil and refrigerants.

2. Experimental apparatus and method

2.1 Quantification technique

Shapes of most of oil droplets inside the upper part of the compressor are spheres. Thus, the beam can be reflected and refracted for all of directions after passing through the droplets. Those reflected and refracted beams have been captured by the CCD camera as shown by Fig. 1. Because the parts of the oils give bright im-

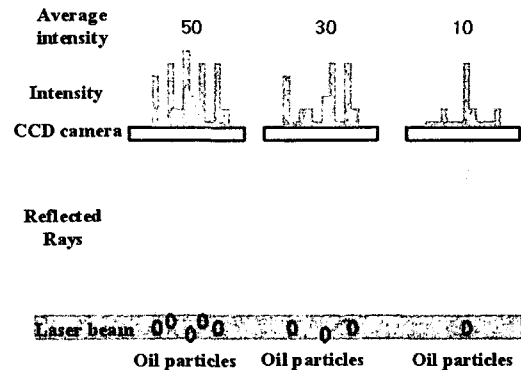


Fig. 1 Principle of quantification of intensity.

ages on the screen, the intensity of the brightness for the image increases if the amount of the oil increases. By this technique, the average intensities of the captured images can be obtained and the amount of the oil inside the compressor can be calculated from the intensities. The average intensity I_{avg} can be derived as follows:

$$I_{avg} = \frac{\sum_{i=0}^{M \times N} I(i)}{256 * (M \times N)} \times 100\% \quad (1)$$

where M and N are numbers of pixels in x and y directions, respectively for an interrogation area and the maximum value of the CCD camera for the 8 bit system is 255 in Eq. (1).

For the test model, most parts of the calculated area are relatively dark including the noise which can increase the error of the calculated values because there is a very small amount of oil inside the test model. Thus, the intensity value has been determined to be 0 if it is lower than the minimum standard, and the average intensity has been calculated using the higher values compared with the standard. Thus, the average intensity of the test model has been obtained using the ppm unit as follows:

$$I_{avg} = \frac{n_{oil}}{256 * (M \times N)} \times 10^6 \text{ (ppm)} \quad (2)$$

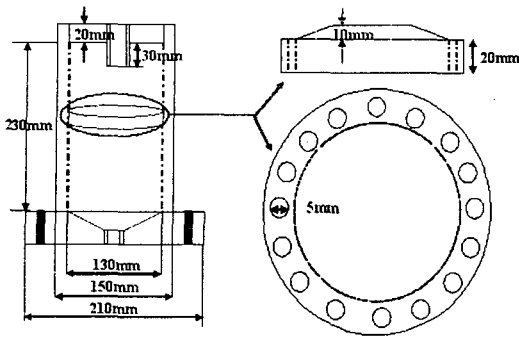


Fig. 2 Layout of test model.

where n_{oil} is a peak point of the calculated area, which is the sum of the intensity values of all pixels where the oil droplets exist.

2.2 Test model

The test model has been manufactured to

obtain projected data from a laser because it is difficult to capture the oil movements inside the real compressor at various conditions. Since the model has been made of acrylic, the whole parts of the exit nozzle can be visualized to analyze average intensities of captured images as shown in Fig. 2. The test model includes a circular plate with many holes with diameters of 5 mm to make similar phenomena as the oil behaviors in the cut-core part of the real compressor. The inserted oil moves upward rapidly through the holes (Fig. 2) like the real compressor.

The amounts of mineral oil and R22 refrigerant can be controlled by an oil generator and a regulator, respectively before inserting to the model so that the total amount of oil and refrigerant inside the test model can be known variables during the experiment (Fig. 3). Also, a

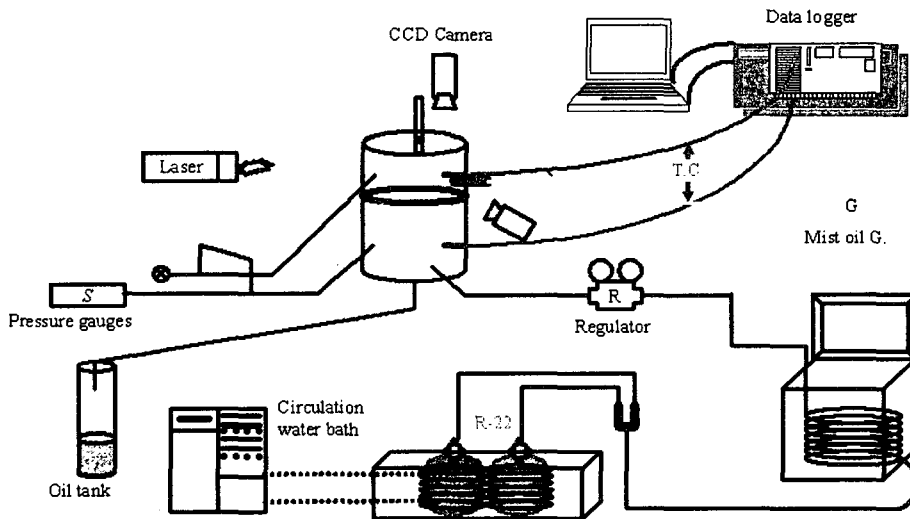


Fig. 3 Experimental setup for test model.

Table 1 Average intensity with inserted refrigerant and discharged oil for test model

Condition	Inserted refrigerant (kg)	Discharged oil (Q_E) (ml)	Average intensity (ppm)
1 atm, 77°C	4.06	7	5502
2 atm, 77°C	6.60	10	8850
1 atm, 57°C	4.12	2	2865
2 atm, 57°C	6.22	7	6686

heating circulator and a thermostat have been installed to control the temperature of the inserted refrigerant. The test model has been visualized by a 80 mW Ar-Ion laser to analyze the oil behavior with known amounts of oil and refrigerant.

The experiment for the test model has been carried out for 4 cases with two different inlet pressures and two different internal temperatures in Table 1. The test model has been investigated by a vertical sheet and a horizontal sheet of the laser beam using a cylindrical lens. The oil has stagnated initially in the hole because of the viscosity, and the oil mists with diameters of 0.1 to 1 mm have appeared from the increase of the momentum of the refrigerant by the difference between upper and lower pressures. The amount of exhausted oil Q_E has been calculated by measuring the amounts of inserted oil Q_I and remained oil Q_R using a scale as follows:

$$Q_E = Q_I - Q_R \quad (3)$$

where Q_I has been fixed to be 60 ml uniformly.

2.3 Rotary compressor for visualization

There are a motor and a cylinder inside the rotary compressor covered by opaque metals as shown in Fig. 4. Thus, a special manufacture by design change should be required to visualize inside the compressor using the laser. In this study, three visualizing windows have been installed to inspect the upper part of the compressor for visualization of the exhausted oil. The windows are made of quartz glass for one ring-shaped window to capture side view and two circular windows for cross-sectional views installed at top plate of the compressor as shown in Figs. 4 and 5. The quartz glasses have been tested for safety and confirmed to be hold until 60 bars that is three times of a real operating condition. Nevertheless, the win-

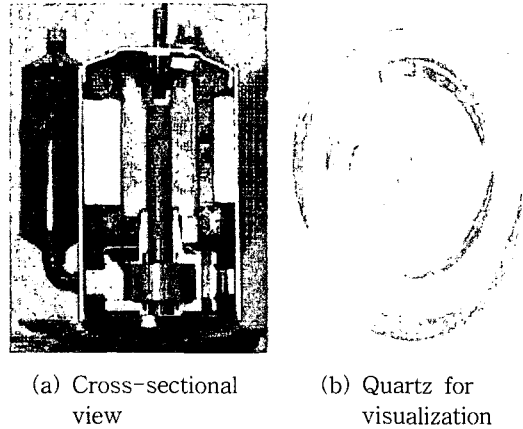


Fig. 4 Photographs of rotary compressor.

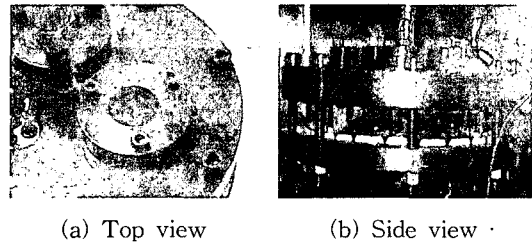


Fig. 5 Photographs of rotary compressor with visualization window.

dow has been covered by polymer film of 0.2 mm to protect from an impact.

The experimental condition has been divided into 3 cases. The average intensities have been observed with various inlet temperatures and outlet pressures of the compressor for case I, various outlet pressures and outlet temperatures for case II, and various operating conditions for case III. Figure 6(a) shows the experimental setup for case I. The vertical sheet of the laser beam has been constructed by the cylindrical lens to capture the side view while the top view has been captured by the horizontal sheet of the white light to avoid the distortion of the images from the interference between two laser beams. The horizontal sheet has been produced to obtain more accurate images (Fig. 6(b)) with various outlet pressures and temperatures of the compressor by only

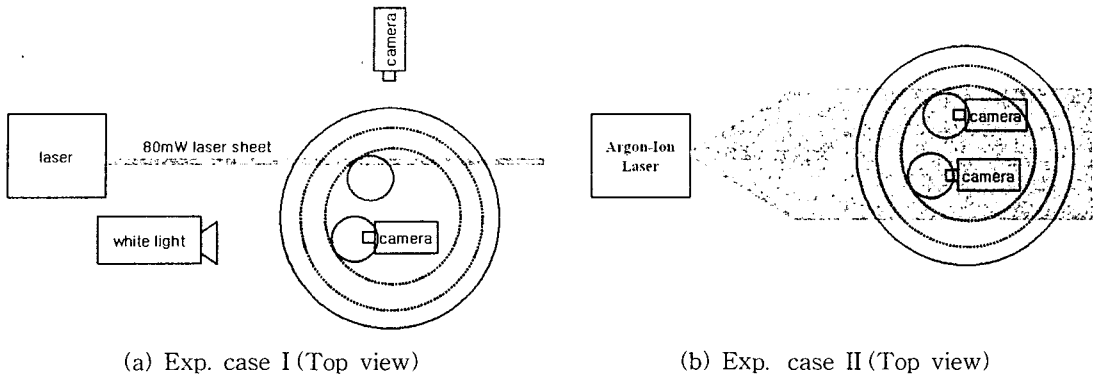


Fig. 6 Schematic diagram for experiment.

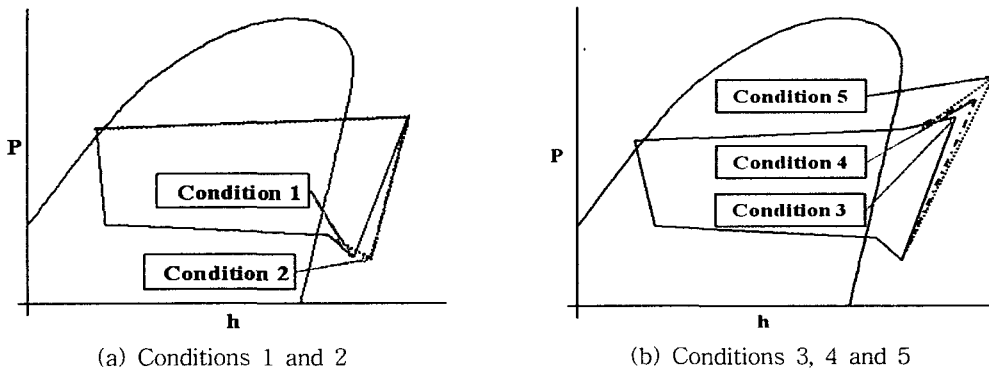


Fig. 7 Cyclomatic chart of case I.

the laser for case II. The CCD camera has been changed and the power of the laser has increased 15 mW for case III with various conditions of refrigeration efficiency test to investigate the reliability of the rotary compressor. Figure 7 shows the cyclomatic chart of each condition for case I.

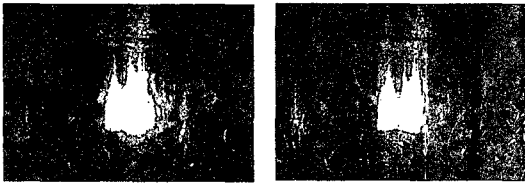
In order to capture the images for cases I and II, a CCD camera (XC-55, Sony) with a resolution of 640×480 has been used. For case III, another camera (HR70C, Sony) with 1024×768 resolution has been used to reduce the noise because the case III has more various conditions and the small changes for the conditions should be detected by the high-resolution camera. The exposed time is $1/1,000$ sec and the aperture number of the lens is $f/8$ for all experiments.

3. Results and discussion

3.1 Test model

The results of the experiment for the test model show that the amount of the exhausted oil and the average intensity inside the upper part of the model increases with increasing the temperature and the pressure of the inserted refrigerant as shown in Table 1 because the oil viscosity has decreased rapidly with increasing the temperature. Also, it has been observed that the average intensity and the exhausted oil increases with increasing the amount of the oil droplets around the exit nozzle.

Figure 8 shows the oil behaviors captured by the CCD camera inside the test model with changing the pressure. The amount of the oil



(a) 1 atm (b) 2 atm

Fig. 8 Oil behaviors by inlet pressure.

particles around the exit nozzle has increased as the inlet pressure increases. The mist oil which has been injected upward from the edge has shown the parabolic orbit and it has been exhausted with the refrigerant through the exit nozzle by the drag force from the refrigerant flow.

3.2 Rotary compressor

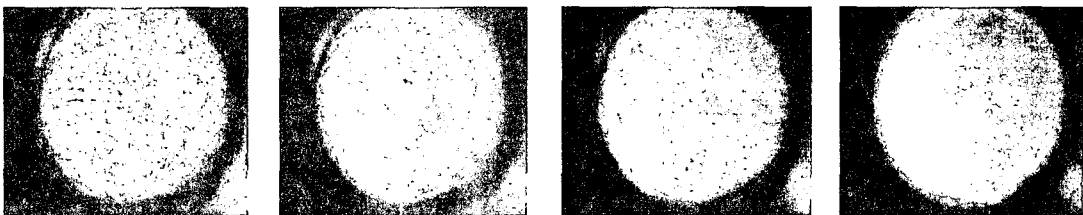
The variation of the average intensity of case I has been shown in Table 2 with change of inlet temperature, outlet temperature and pressure. There is not much change for the intensity by the inlet temperature of the re-

frigerant while the intensity has increased as controllable and independent variables such as the outlet pressure and temperature of the compressor increases. The average intensity inside the test model has varied by the inlet temperature because the viscosity of the oil decreases greatly with increasing the inlet temperature for the ambient condition. Thus, many oil droplets have appeared in the upper part of the model. However, the experiment for the real compressor has been performed at the high temperature condition where the change of the viscosity is relatively small. Thus, the variation of the average intensity is not large by the inlet temperature. Figure 9 shows the captured image of case I. The circular spot in the image is the attached oil to the visualization window and it has been excluded for the calculation. From the results, it is realized that the amount of the oil is influenced more by the outlet pressure than by the inlet temperature because the image is brighter for the condition of high pressure (Fig. 9).

The effect of the outlet pressure and tem-

Table 2 Average intensities with various conditions for rotary compressor (case I)

	Inlet temperature (°C)	Outlet temperature (°C)	Outlet pressure (atm)	Average intensity of top view (%)	Average intensity of side view (%)
Condition 1	26.3	89.3	11.8	53.1	60.1
Condition 2	30.0	90.6	11.9	53.2	60.5
Condition 3	29.6	95.6	13.1	56.4	60.8
Condition 4	30.0	106.1	16.2	60.8	64.9
Condition 5	30.1	123.6	20.7	75.3	76.3



(a) Condition 1 (b) Condition 2 (c) Condition 3 (d) Condition 5

Fig. 9 Captured images of case I.

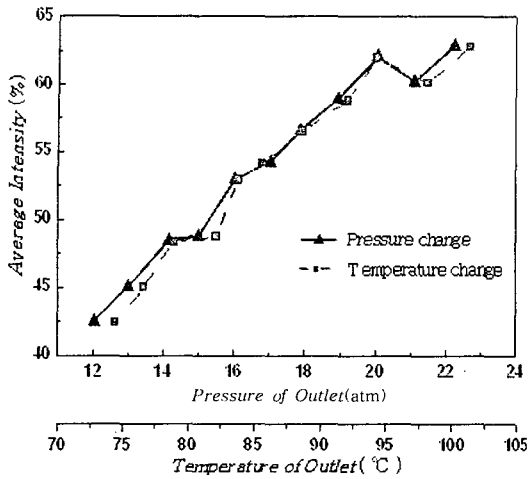


Fig. 10 Average intensity of rotary compressor with outlet temperature and pressure (case II).

perature have also been investigated by the average intensity using case II. The average intensity increases with increasing the outlet pressure and temperature as shown in Fig.10. It is realized that the major factor of the average intensity change is the outlet pressure because increase of the outlet temperature causes increase of the outlet pressure. If the outlet pressure increases, the internal pressure difference and the velocity of the refrigerant increase and more oil droplets can be jetted upward.

The case III has been carried out for various

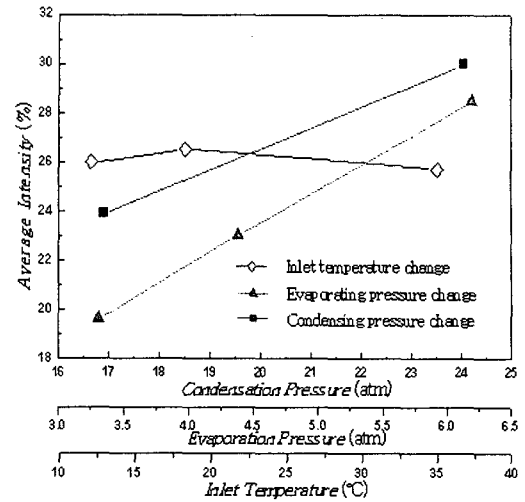


Fig. 11 Average intensity of rotary compressor with outlet temperature evaporation and condensation pressure (case III).

conditions of refrigeration efficiency test especially for the condensing pressure (P_c) and the evaporating pressure (P_e) to investigate the average intensity of the rotary compressor as shown in Table 3. Although the intensities inside the rotary compressor have not been affected by the inlet temperature (T_s) greatly as shown by Fig. 11, those increase as the outlet (condensing) pressure increases like the results of the cases I and II. In case III, it has also been observed that the intensities increase rapidly with increasing the evaporating pressure

Table 3 Conditions and average intensities for case III

No	Name	Parameter	P_e (atm)	P_c (atm)	T_s (°C)	Intensity (%)
1	ASHRAE-T	Standard	6.4	21.9	35.0	25.7
2	ARI	T_s	6.4	21.9	18.3	26.6
3	ARI-low suction temp		6.4	21.9	9.2	25.9
4	A/C cooling standard		6.9	17.6	15.0	28.0
5	High condensing pressure	P_c	6.4	24.8	35.0	30.7
6	Low condensing pressure		6.4	17.6	35.0	23.9
7	High evaporating pressure	P_e	6.9	21.9	37.8	28.5
8	Low evaporating pressure		5.1	21.9	27.8	22.9
9	Ultra-low evaporating pressure		3.6	21.9	17.8	19.6

which can be a controllable and independent variable.

4. Conclusions

The conclusions from the analysis of the oil behaviors in the test model and the rotary compressor using the developed visualization technique have been obtained as follows:

(1) The relationship between the amounts of the exhausted oil and the remained oil around the exit nozzle has been derived from the analysis of the oil behaviors in the test model and the rotary compressor using the visualization technique, and the quantitative study has been proposed in this study.

(2) If the refrigerant in the gas state is inserted into the rotary compressor, the average intensity at the upper part of the compressor has not been affected much by the inlet temperature.

(3) The major factor for the change of the average intensity inside the compressor is the outlet pressure and the evaporating pressure which are the independent variables.

(4) The mechanism of the exhausted oil has been observed and the quantitative measurement has been performed using the test model, which is difficult for the real compressor.

Acknowledgement

This work was supported by grant No. 2004-0687-600 from Smart Future Appliances Research Center (SFARC).

References

1. So, S.K., Lee, S.K. and Pack, Y.S., 1998, Rotary compressor for air-conditioning, Fluid Machinery J., Vol. 1, pp.106-112.
2. Lee, J.B. and Lee, S.K., 2003, Correlation analysis between OCR and differential pressure of rotary compressor, Proceedings SA-REK 2003, Summer, pp. 700-704.
3. Kim, H.S. and Katsuta, M., 1995, Influence of refrigerant oil on evaporator performance, Trans, JAR, Vol. 12, No. 1, pp. 1-24.
4. Parkash, N. and Pandeya, P., 1986, A simplified procedure for designing hermetic compressors, Purdue Comp. Conf., pp.415-427.
5. Asanumza, H., Itami, T. and Ishikawa, H., 1984, An experimental study of the shaft oil supply mechanism of a rotary compressor, Proceedings the International Compressor Engineering Conference, Purdue, pp.383-390.
6. Takebayashi, M., Iwata, H. and Sakazume, A., 1988, Discharge characteristics of an oil feeder pump using nozzle type fluidic diodes for a horizontal compressor depend on the driving speed, Proceedings the International Compressor Engineering Conference, Purdue, pp.19-26.
7. Kim, K. and Cho, K., 1988, A study on lubricating system of hermetic rotary compressor, Proceedings the International Compressor Engineering Conference, Purdue, pp.27-33.
8. Ko, H.S. and Kim, Y.J., 2003, Tomographic reconstruction of two-phase flows, KSME Int. J., pp.571-580.